Materials Science and Technology

ISSN: 0267-0836 (Print) 1743-2847 (Online) Journal homepage: http://www.tandfonline.com/loi/ymst20

Vanadium microalloying for ultra-high strength steel sheet treated by hot-dip metallising

B. Hutchinson, D. Martin, O. Karlsson, F. Lindberg, H. Thoors, R. K.W. Marceau & A. S. Taylor

To cite this article: B. Hutchinson, D. Martin, O. Karlsson, F. Lindberg, H. Thoors, R. K.W. Marceau & A. S. Taylor (2017) Vanadium microalloying for ultra-high strength steel sheet treated by hot-dip metallising, Materials Science and Technology, 33:4, 497-506, DOI: 10.1080/02670836.2016.1235841

To link to this article: http://dx.doi.org/10.1080/02670836.2016.1235841

Vanadium microalloying for ultra-high strength steel sheet treated by hot-dip metallising

B. Hutchinson*[1], D. Martin[1], O. Karlsson[1], F. Lindberg[1], H. Thoors[1], R. K.W. Marceau[2] and A. S. Taylor[2]

Ultra-high strength steel sheets have been subjected to heat treatments that simulate the thermal cycles in hot-dip galvanising and galvannealing processes and evaluated with respect to their resulting mechanical properties and microstructures. The steels contained suitable contents of carbon (~0.2%), manganese (1.2%) and chromium (0.4%) to ensure that they could be fully transformed to martensite after austenitisation followed by rapid cooling in a continuous annealing line, prior to galvanising. Different contents of vanadium (0–0.1%) and nitrogen (0.002–0.012%) were used to investigate the possible role of these microalloying elements on the strength of the tempered martensite. Vanadium, especially when in combination with a raised nitrogen content, helps to resist the effect of tempering so that a larger proportion of the initial strengthening is preserved after the galvanising cycle, giving tensile strength levels exceeding 1000 MPa. Different deoxidation practices using aluminium or silicon have also been included. These showed similar strength levels at corresponding carbon contents but the bendability of the Si-killed steel sheet was considerably superior. Microstructural examinations have been made on the annealed steels but the reason for the beneficial effect of vanadium is still not fully explained. It is concluded that microalloying with vanadium is a very promising approach in the development of corrosion-resistant ultra-high strength steel sheet products.

Keywords: Sheet steel, Vanadium, Galvanising, Galvanealing, Strength, Ductility, Bendability, Microstructures

Introduction

Demands to save energy and limit CO_2 emissions are driving manufacturers to adopt materials with ever higher strength levels for vehicle construction and building materials in order to save weight. Grades such as dual phase, complex phase and TRIP steels are increasingly being used but for even greater strength it is necessary to turn to bainitic and ultimately martensitic structures. Already today, ultra-high strength martensitic steel sheets are produced with usable formability and with tensile strength levels in the range 1000–1600 MPa.[1] However, in addition to the needs for strength and formability, these materials must also be protected against corrosion. The usual practice at present is to use electrolytic galvanising but this poses a number of problems. First, it is more expensive than conventional hot-dip galvanising and the maximum achievable coating masses are generally lower. The electrolytic process is also prone to charging the steel with hydrogen which is well known to pose risks of delayed fracture in higher strength grades. In addition, galvannealing is preferred over zinc galvanising in many applications from the viewpoint of paint adhesion, painted appearance and underfilm corrosion resistance.[2,3] The aim of the present work was, therefore to investigate alternative possibilities for manufacturing ultra-high strength steels suitable for coating with existing hot-dip lines.

The obvious problem that arises with a hot metallising process is that martensite will become tempered and lose much of its strength. Temperatures necessary for hot-dip galvanising baths, ~460°C, are significantly higher than those for tempering in typical continuous annealing lines so loss of strength is to be expected. The effect of different alloy elements has been extensively studied in engineering steels with respect to temper-resistance and the occurrence of secondary hardening. One such element that is known to be most effective in this regard is vanadium[4] and for this reason it was chosen in the present investigation. Experience with bainitic strip steel has also demonstrated that vanadium acts to stabilise the strength at elevated temperatures.[5] In most microalloying applications, the effect of vanadium is found to be augmented when used in combination with nitrogen since VN is a more stable phase than VC in steel.[6] Although the situation in martensitic structures differs in many ways from the ferrite-pearlite-bainite in HSLA structural steels, it was considered of interest to see whether the nitrogen content is also relevant in the present circumstances.

[1]SwereaKIMAB, Kista, Box 7047 SE-164 07, Sweden
[2]Deakin University, Institute for Frontier Materials, Geelong 3216, VIC, Australia

*Corresponding author, email bevis.hutchinson@swerea.se

Received 27 July 2016; accepted 3 September 2016
DOI 10.1080/02670836.2016.1235841

Experiments were designed to investigate the influence of different vanadium and nitrogen contents and also to see what strength levels could be achieved through adjustment of the carbon content within the range that is typical for ultra-high strength sheet. Following a hardening treatment of austenitisation and quenching, subsequent anneals were carried out to simulate the thermal cycles implied by a hot-dip metallising process. This did not involve actual zinc coating; our findings refer only to the properties and structures of the steel itself. Although the time spent in the zinc bath by a sheet is normally only of the order of seconds, the sheet temperature must be raised first in a strand-annealing furnace which typically takes a few minutes. Most of the results described here refer to an anneal of 5 minutes at 460°C but a shorter time of 10 seconds was also investigated to see the possible effect of an alternative rapid anneal as, for example, by transverse flux induction heating. Some of the samples were studied in this 'galvanised' condition while others were given an additional heat treatment of 15 seconds at 550°C[7] to generate a 'galvannealed' condition. The resulting materials were examined by tensile and bend testing and by metallography.

Experimental procedure

The experimental programme was carried out in two stages. First, a series of six melts were made to investigate the effects of varying the vanadium and nitrogen contents in aluminium-deoxidised steels with fixed levels of carbon and other elements. Then a further three melts were made with varying carbon contents using silicon additions rather than aluminium for deoxidation. The melts of approximately 2 kg were processed in a vacuum induction furnace and cast into square section, 40 × 40 mm, moulds. After cutting off any pipe at the top and a slice for chemical analysis at the bottom, the ingots were about 150 mm in length. These were first hot rolled to 4 mm thickness, finishing around 900°C and air cooled. After removal of the scale, the sheets were cold rolled to 1.1 mm.

Tensile specimens having a free length of 60 mm and bend test coupons 40 × 60 mm were machined from the sheets. The long axes of these specimens were along the rolling direction and the bend tests were arranged with the bending axes in the transverse direction. Heat treatments for hardening the steels were done at 900°C in a muffle furnace for 3 minutes followed by quenching vertically into water. A preliminary investigation showed that the specimens reached a temperature of 890°C within 90 seconds. Further heat treatments were done in a salt bath. To simulate a typical galvanising line the specimens were held for 5 minutes at 460°C but for a possible shorter induction heating process, this was reduced to only 10 seconds. Half of these samples were retained for testing while the others were given a second salt bath treatment of 15 seconds at 550°C, corresponding to a typical galvannealing process, although not identical in view of the intermediate cooling to room temperature.

Tensile testing was carried out in an Instron universal machine to provide values of the yield stresses (Rp) and tensile strengths (Rm) as well as uniform and total elongations (Ag and Atot) based on a 50-mm gauge length extensometer. Quoted results are averages of the values for two or sometimes three specimens. Critical bending conditions were measured in three-point loading according to German standard VDA238. In this method the supports rotate on bearings to minimise friction effects and the bending tool has a sharp radius of 0.4 mm. The separation distance of the supports used with these 1 mm sheet materials was 32.5 mm. A small pre-load of 30N was applied to define the starting point after any initial buckles in the specimen had been removed. The punch travel length L up to the maximum load, measured in millimetres, is a measure of bendability from which the critical bend angle β can also be derived.

Metallographic examination was first performed with EBSD maps derived from measurements in Zeiss Supra field emission gun scanning electron microscope using Oxford HKL software to give measures of mean linear intercepts for lath boundaries and prior austenite grain (PAG) sizes. The lath boundary spacings were evaluated at different threshold misorientations between 3° and 15°. The PAG sizes were determined from boundaries having misorientations in the interval 18–47° where there is no interference from the martensite structure. To compensate for 'lost' PAG boundaries that lay outside this range the number of intersections was increased by 59% based on the Mackenzie distribution for random orientations which is believed to be a fair approximation in the present situation. X-ray diffraction was applied to investigate any differences in recovery of the martensite structure as a result of the annealing. Line breadths for the (110) and (220) reflections were analysed using the Hall-Williamson method as described elsewhere[8,9] to give a measure of internal strains and dislocation content.

A Jeol JEM-2100F field emission gun transmission electron microscope was applied in selected cases to get improved resolution images of substructures and particles if present. This was done using thin foil specimens made by electro-polishing. Electron imaging was complemented with high resolution EDS X-ray mapping.

Specimens for atom probe tomography (APT) were prepared by first cutting small blanks (~0.25 mm × 0.25 mm × 15 mm) from the sheet material and these were then sharpened into needle-like specimens having very fine tips (radius ~50–100 nm) by a standard two-stage electro-polishing technique,[10] using electrolytes of 10% perchloric acid in undiluted ('glacial') acetic acid and 2% perchloric acid in 2-butoxyethanol for the 1st and 2nd stages, respectively. Atom probe experiments were conducted using a Local Electrode Atom Probe 4000 HR instrument (CAMECA Instruments Inc.) operating in voltage mode under ultra-high vacuum at a set-point temperature of 60 K, pulse fraction of 20%, pulse repetition rate of 200kHz, detection rate of 0.005 atoms per pulse. Tomographic reconstruction and visualisation of the APT data was performed with the IVAS 3.6.8 software. It is noted that the mass spectra display peak overlap, namely between Cr^{2+}, Fe^{2+} and Al^{+} ions at mass-to-charge-state ratio of 27 Da. Reported bulk compositions have therefore been obtained after peak decomposition based on the natural abundance of isotopes, using the built-in function within the IVAS software.

Results and discussion

Chemical analyses of the ingots are presented in Table 1. The manganese and chromium contents were selected to provide sufficient hardenability such that these steels could be made fully martensitic in lines employing gas

Table 1 Chemical compositions of the steels in wt-%. Al_{sol}, N_{sol} and V_{sol} are solid solution contents at 900°C calculated using ThermoCalc

Steel code	C %	Si %	Mn %	Cr %	Al %	V %	N %	Al_{sol} %	V_{sol} %	N_{sol} %
1. 0 V/LN	0.200	0.013	1.203	0.392	0.022	0.001	0.0025	0.017	0.001	0.0006
2. 0 V/HN	0.194	0.016	1.217	0.392	0.023	0.001	0.0125	0.003	0.001	0.0032
3. LV/LN	0.200	0.008	1.226	0.399	0.026	0.050	0.0027	0.020	0.050	0.0005
4. LV/HN	0.196	0.010	1.172	0.392	0.021	0.048	0.0126	0.005	0.036	0.0023
5. HV/LN	0.200	0.009	1.224	0.387	0.029	0.097	0.0025	0.023	0.097	0.0007
6. HV/HN	0.199	0.013	1.176	0.389	0.021	0.092	0.0125	0.009	0.062	0.0013
7. LV/LC	0.152	0.264	1.235	0.398	0.003	0.052	0.0072	0.003	0.032	0.0024
8. LV/NC	0.201	0.265	1.232	0.399	0.003	0.051	0.0071	0.003	0.031	0.0025
9. LV/HC	0.251	0.258	1.224	0.395	0.003	0.051	0.0080	0.003	0.029	0.0028

jet cooling as well as water cooling. Apart from the intentional variations in vanadium and nitrogen, the alloying elements were maintained at very uniform levels. For better clarity, abbreviated steel codes have also been included where 0 V means reference steels without vanadium, LV is low vanadium, HV is high vanadium, LN is low nitrogen and HN is high nitrogen. For steels 7–9, LC, NC and HC are low, normal and high carbon levels. In addition to the total elemental contents, Table 1 also gives the contents of aluminium, vanadium and nitrogen that are dissolved in

Table 2 Summary of mechanical test results.

Steel	Time at 460°C	Time at 550°C	Rp MPa	Rm MPa	Ag %	Atot %	Bend depth mm	Bend angle degrees
1	0	0	1147	1521	2.4	5.4	6.72	58
1	5 min	0	965	1019	3.5	6.3	8.82	82
1	10 sec	0	1094	1170	2.5	5.1	8.67	80
1	5 min	15 sec	910	952	3.6	6.5	9.37	88
1	10 sec	15 sec	907	945	3.6	6.5	9.64	92
2	0	0	1137	1537	2.9	4.9	6.00	51
2	5 min	0	1030	1073	3.4	6.3	6.76	59
2	10 sec	0	1126	1198	2.6	5.3	7.30	65
2	5 min	15 sec	995	1030	3.9	6.8	6.82	59
2	10 sec	15 sec	1004	1038	4.0	7.0	7.23	64
3	0	0	1147	1540	2.9	4.8	6.38	55
3	5 min	0	1006	1064	3.1	6.1	7.91	71
3	10 sec	0	1080	1169	2.5	5.0	7.84	70
3	5 min	15 sec	938	988	3.5	6.4	8.16	74
3	10 sec	15 sec	936	985	3.3	6.1	8.36	76
4	0	0	1147	1556	3.1	5.1	5.59	47
4	5 min	0	1037	1094	2.7	5.1	6.05	51
4	10 sec	0	1159	1217	2.4	5.0	6.22	53
4	5 min	15 sec	1038	1068	3.3	5.9	6.22	53
4	10 sec	15 sec	1027	1060	3.4	6.0	6.46	56
5	0	0	1149	1532	2.3	4.2	6.57	57
5	5 min	0	1032	1089	2.9	5.6	8.09	73
5	10 sec	0	1108	1188	2.6	5.4	8.04	73
5	5 min	15 sec	969	1016	3.2	6.0	8.01	72
5	10 sec	15 sec	985	1019	3.3	6.6	8.61	79
6	0	0	1204	1606	3.1	5.9	6.36	54
6	5 min	0	1124	1133	0.3	3.3	6.94	61
6	10 sec	0	1211	1231	2.2	4.8	7.02	61
6	5 min	15 sec	1079	1099	0	3.4	7.61	68
6	10 sec	15 sec	1082	1091	0	3.5	7.87	71
7	0	0	1031	1362	3.6	6.2	7.87	91
7	5 min	0	992	1025	2.9	5.5	>12.22	>126
7	10 sec	0	1065	1120	2.5	4.8	>12.81	>139
7	5 min	15 sec	985	995	2.7	5.2	>13.00	>134
7	10 sec	15 sec	985	995	2.7	5.2	>13.00	>137
8	0	0	1167	1546	3.2	5.8	9.86	94
8	5 min	0	1059	1093	3.1	5.8	>12.35	>128
8	10 sec	0	1115	1183	2.8	5.4	>13.11	>133
8	5 min	15 sec	1038	1058	3.1	5.6	>12.34	>127
8	10 sec	15 sec	1032	1053	3.6	6.3	>12.45	>129
9	0	0	1247	1720	2.7	4.8	8.60	79
9	5 min	0	1117	1147	3.1	5.8	>12.73	>133
9	10 sec	0	1122	1274	2.3	4.9	>12.75	>129
9	5 min	15 sec	1064	1117	3.6	6.4	>12.64	>132
9	10 sec	15 sec	1093	1117	3.8	6.8	>12.39	>130

All specimens heated at 900°C for 3 minutes and water quenched, followed by various salt bath heat treatments as indicated.

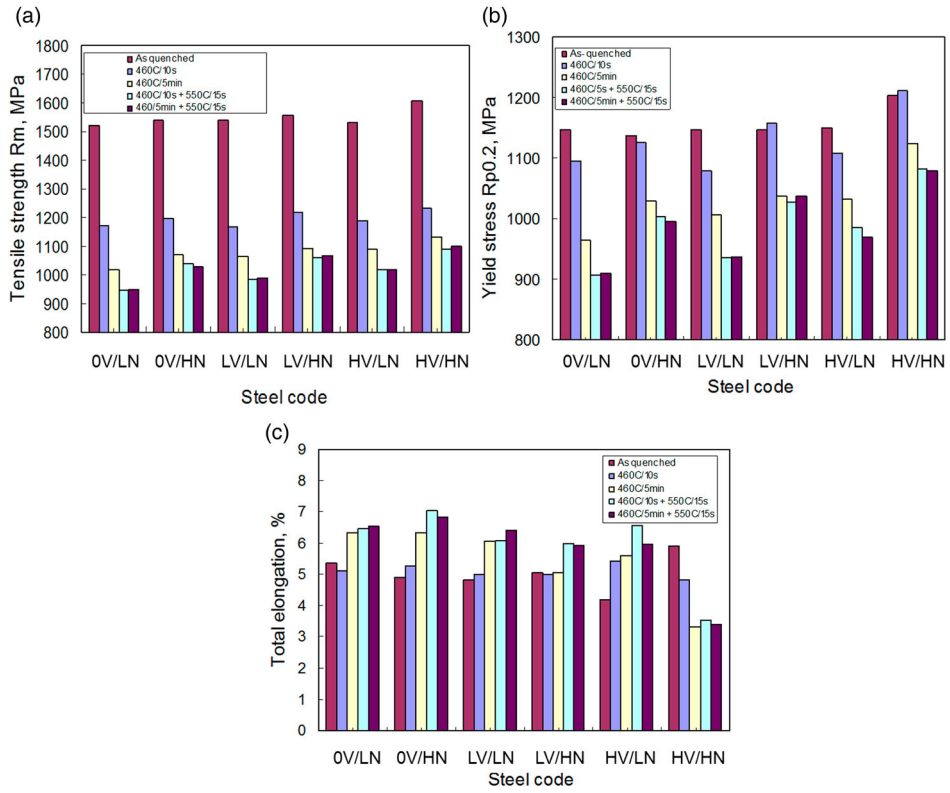

1 Summaries of tensile test properties for the 0.2%C steels 1–6 after various heat treatments to simulate galvanising and galvannealing processes, *a* yield stress, *b* tensile strength and *c* total elongation

the austenite at the hardening temperature of 900°C, as calculated using ThermoCalc. These values may be more relevant to the tempering process since prior precipitates of AlN and VN are unlikely to play any role.

All tensile test data are summarised in Table 2. However, most of the subsequent discussion will be restricted to the 5 minute heat treatments at 460°C which approximate most present-day hot-dip galvanising lines. The shorter, 10 second, treatments apply to a hypothetical rapid annealing process and these results will only be described briefly in the following text. Figure 1 shows the average values for (a) 0.2% proof stress (Rp), (b) tensile strength (Rm) and (c) total elongation (Atot) in the form of bar charts for steels 1–6, all having 0.2%C, in the various heat treated conditions. In the as-quenched condition the yield and tensile strengths vary very little with composition. There is a small influence of nitrogen content which may be due to its acting as surrogate carbon; if the extra 0.01%N were equivalent to carbon it would occasion about 40 MPa increase in tensile strength.[11] The short time (10s) annealing at 460°C decreases the tensile strength markedly but leaves the proof stress values almost unchanged as is commonly the case with mild tempering treatments.[9] However, the more relevant 5 minute anneals not only reduced further the tensile strengths but also lowered the proof stresses by about 100 MPa. The additional treatment of 15s at 550°C led to further reductions in both yield and tensile strength. After this treatment, there was almost no residual effect of the previous annealing time at 460°C which implies that any benefits of a new ultra-rapid annealing process would be negligible after galvannealing. The simulated galvanising and galvannealing treatments generally raised the total elongation values by about 1% although not for steel 6 where ductility was reduced. In this case instability occurred immediately on yielding in tension with no uniform elongation.

The most interesting observations are the increased strength that results from alloying with vanadium and also with nitrogen after heat treatment. The tensile strength values and, especially, the yield stresses are seen in Fig. 1 to rise with increasing alloy content after both the simulated galvanising and galvannealing treatments, despite their being virtually constant in the as-quenched conditions. The total elongations are almost the same for all the materials excepting steel 6. These results point to a potentially useful role of vanadium in ultra-high strength steels that require galvanising. They also show that, just as in other HSLA steels,[6] a raised nitrogen content plays a synergistic role together with vanadium. This is seen better in Fig. 2*a* where the yield and tensile values are plotted as a function of the product of the vanadium and nitrogen contents of the steels. It is not sure that the most highly alloyed condition can be used in practice due to its inferior ductility but, even ignoring these results, the tensile strengths are raised by 50–100 MPa and the yield stresses by more than 100 MPa. According to some steel specifications[1] there is a critical requirement for the tensile strength to exceed 980 MPa which can be reliably achieved with this V-N-microalloying.

It would be expected that vanadium can only be effective for inhibiting tempering when present in solid solution since it otherwise occurs in rather coarse precipitates of vanadium nitride, VN. The contents of active vanadium on this basis were calculated assuming equilibrium is reached in the austenitising treatment at 900°C, as shown in Table 1. Simple correlation of strength

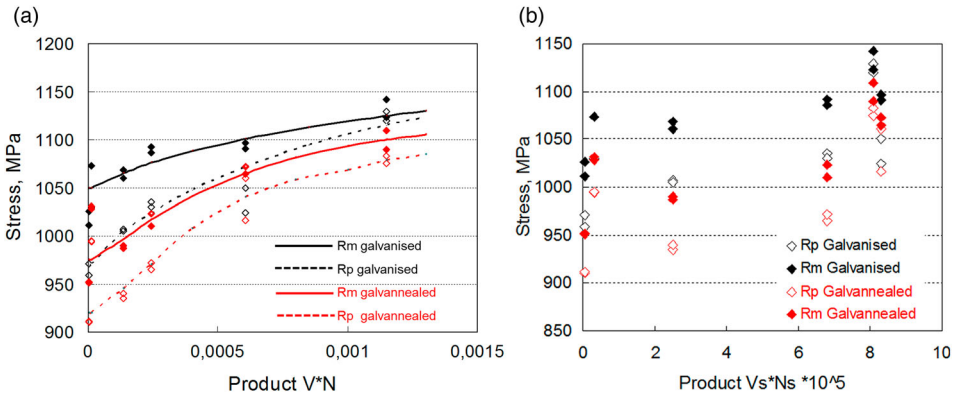

2 Yield and tensile stress values for 0.2%C steels 1–6 plotted as a function of the product of vanadium and nitrogen contents in the steels, *a* total contents, *b* soluble contents

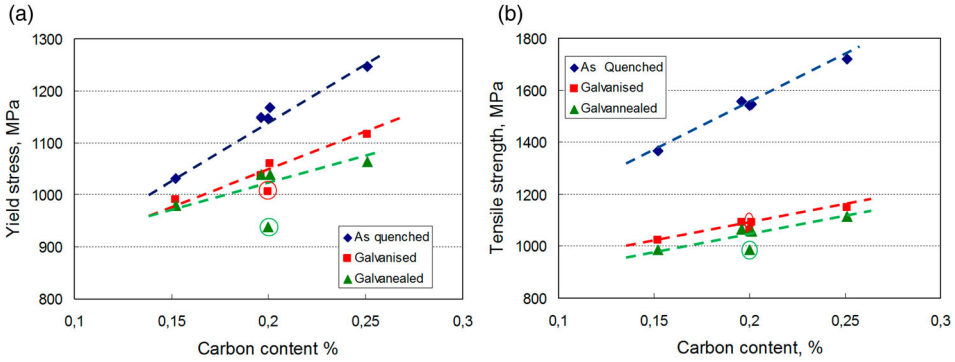

3 Tensile test results for steels containing 0.05%V with different carbon contents, *a* yield stress, Rp, *b* tensile strength, Rm. Data points for the annealed low nitrogen steel 3 are shown circled

after tempering with solute vanadium, V_{sol}, is very poor but a dependence on V_{sol} together with solute nitrogen, N_{sol}, looks more convincing, Fig. 2*b*. Nevertheless, although a trend is evident here, it is not very rational and one may doubt whether the use of dissolved contents gives any improvement over the total contents shown in Fig. 2*a*.

Further control over strength levels is possible by changing the chemical composition of the steel, in particular with respect to its carbon content. The three steels 7, 8 and 9 were made to examine this possibility at a constant vanadium level of 0.05%. Since no aluminium was added to these melts, nitrogen could not be combined as AlN and therefore the nitrogen level was modified to ~0.007%. Probably a lower level still would be suitable, and even preferable, since the calculations in Table 1 indicate that some of the vanadium would be tied up as VN at the hardening temperature. Strength properties for these steels are shown in Fig. 3 in as-quenched conditions and after simulated galvanising and galvannealing.

Also included in Fig. 3 are values for steels 3 and 4 which have the same vanadium and carbon contents. Strength varies in a linear manner with the carbon contents for all the as-quenched specimens as is normally observed[11] and with a stronger dependence for tensile strength than for yield stress. The influence of carbon level becomes less pronounced after the simulated hot-dipping processes, with the low nitrogen steel LV/LN, shown circled in Fig. 3, deviating significantly from the general trend. This provides further support for the view that vanadium is most effective under these conditions when it is present together with nitrogen.

Bendability measurements are presented in Table 2 and shown graphically in Fig. 4. There is a general tendency for the bendability to deteriorate as strength increases, as expected. In particular, the as-quenched conditions for all steels are significantly inferior when compared to the annealed ones. Higher nitrogen contents in steels 1–6 give poorer bendability, in line with their higher strength. The relationship between tensile strength and

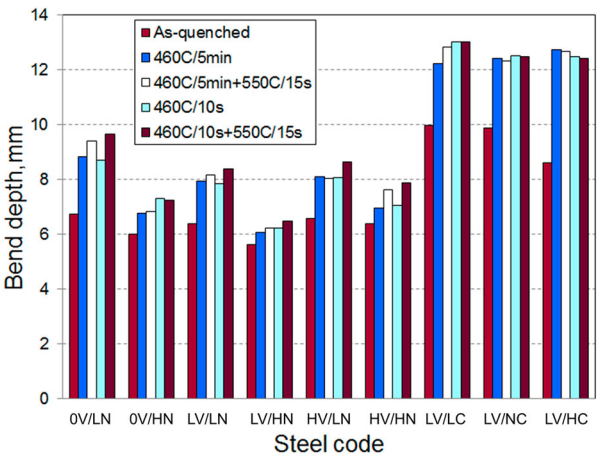

4 Bendability index for the steels in different heat treated conditions

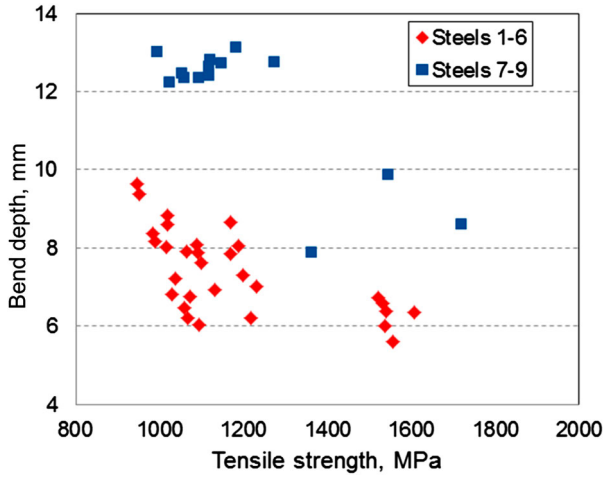

5 Relationship between tensile strength and bendability index

bendability index is shown in Fig. 5. A surprising observation is the superior behaviour of the second series steels 7–9, as compared to the preceding ones, at equivalent strength levels. Note that all the annealed specimens from the latter series bottomed-out in the bending rig so their potential formability should be even higher than the results in Figs. 4 and 5 indicate.

Fracture surfaces for two of the steels, LV/HN and LV/NC, are shown as SEM micrographs in Fig. 6. These represent steels with similar vanadium contents (0.05%V) and equivalent strength levels, where steel LV/HN was aluminium-killed and LV/NC was silicon-killed. Both had shear lips at the outer surface where the fracture is believed to have commenced. This zone was larger in the case of steel LV/NC and there was a notable difference in their appearance. The density of dimples was much greater in steel LV/HN, suggesting that this contained more sites where fracture was initiated. Particles in the larger dimples were typically aluminium oxides and manganese sulphides but it is possible that smaller aluminium nitrides may also have played a role. The silicon-killed steel 8 had far fewer dimples. Particles on this fracture surface were mostly manganese aluminium silicates together with some manganese sulphides. It seems reasonable to deduce that the difference in bendability between the two steel categories is, at least in part, a result of their different contents of second phases.

Various metallographic techniques have been used in order to try to understand the mechanism by which vanadium together with nitrogen resists the loss of strength in these steels during annealing. Some examples from the microscopy are presented in Fig. 7.

The general features of the steels after annealing for 5 minutes at 460°C were typical of tempered martensites, comprising acicular lath-like grains and cementite particles distributed both in the lath and the PAG boundaries and also inside the laths themselves, Fig. 7*a*. No evident difference could be seen between the cementite dispersions of these steels and none would probably be expected. The EBSD map in Fig. 7*b* is typical of lath martensite structures where blocks of approximately parallel laths exist within packets of aligned structures inside the PAGs.

Since misorientations of <3° were not admitted in the pattern analyses, not all the lath boundaries are resolved as can be seen from comparison with the pattern quality map, Fig. 7*c* which is more sensitive in this regard and shows a denser fine scale structure. Finally, PAG boundaries are shown in Fig. 7*d* by misorientations in the range from 18° to 47°. As mentioned above, this network is not complete as it omits any true PAG boundaries with smaller or larger misorientations, but it gives a clear impression of the prior structure and can give a fairly reliable measure of its grain size. Mean linear intercept lengths calculated in this way are shown in Table 3. These austenite grains are generally small, having formed from fine ferrite grain structures during the hardening treatment and stabilised by microalloy nitride particles at 900°C. The steels with high N-contents are consistently finer than those with low N and steel 6 with the greatest amount of VN and AlN has remarkably small PAGs which may have contributed to its higher strength level, even in the as-quenched state.

Mean linear intercept lengths for the internal boundaries in martensite are also given in Table 3, evaluated for two different misorientation criteria, $\Theta > 3°$ and $\Theta > 15°$. There are some differences between the steels but it can be seen that increments between these respective values are rather constant which suggests that the differences are mainly connected with the frequencies of high angle structures such as block or packet boundaries which, in turn, may be linked to the PAG structures. There is, however, a tendency among the steels 7–9 for the martensite structures to become finer with increasing carbon content, in agreement with previous investigations.[12]

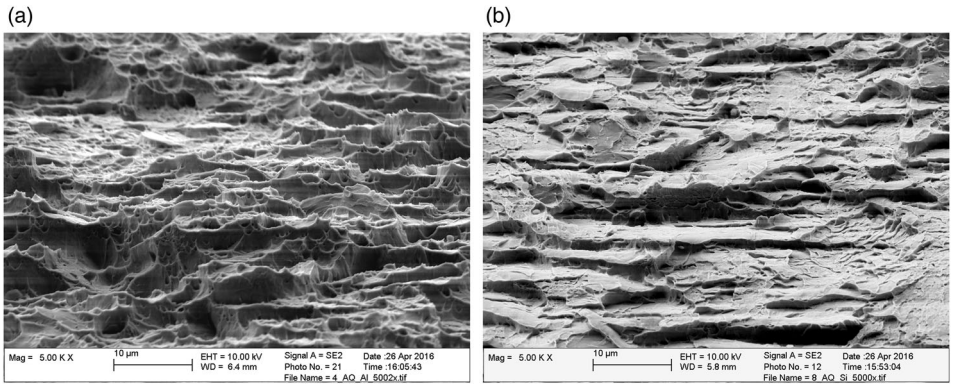

6 Fracture surface below the outer surface of bend specimens for steels 4 (LV/HN) and 8 (LV/NC) in the as-quenched conditions, *a* Al-killed steel 4 and *b* Si-killed steel 8

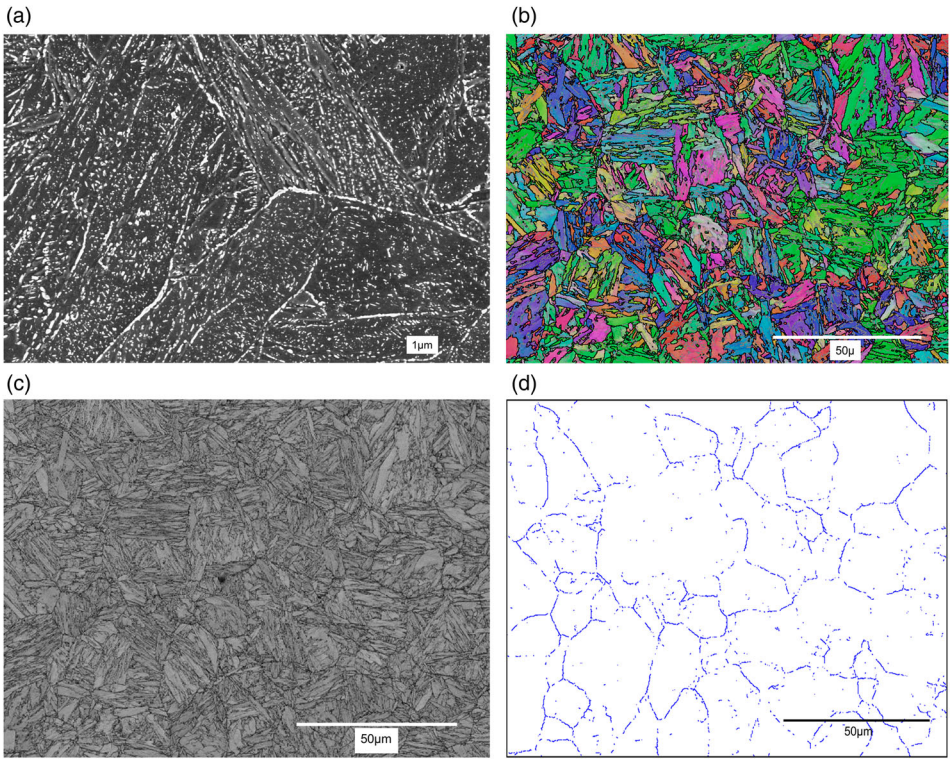

7 Examples of SEM micrographs for steel 4 (LV/HN). *a* secondary electron image, *b* EBSD map using inverse pole figure colouring, *c* EBSD map using band contrast and *d* EBSD map of PAG boundaries having misorientations between 18° and 47°

Table 3 Grain sizes (mean linear intercept lengths in μm) after a simulated galvanising treatment of 460°C for 5 minutes, for PAGs and for martensite boundaries with different criteria for the critical misorientation angle Θ

Steel code	0 V/LN	0 V/HN	LV/LN	LV/HN	HV/LN	HV/HN	LV/LC	LV/NC	LV/HC
PAGs	12	8	15	11	10	5	8	7	6
Martensite Θ > 3°	1.05	0.90	0.92	1.00	0.97	0.80	0.83	0.78	0.70
Martensite Θ > 15°	1.63	1.40	1.44	1.59	1.58	1.20	1.38	1.12	0.99

An attempt to correlate strength levels with these mean linear intercept values for martensite is presented in Fig. 8, based on the Θ > 15° measurements. Although there appears to be a possible relationship here, there are also grounds for believing that it may be illusory. The range of variation is considerable in view of the small interval in grain size and correlation rests heavily on two extreme cases of steels 1 and 6. Additionally, the high angle boundary structures considered here are more likely to be associated with conditions during the hardening treatment, such as PAG size, than the more subtle changes that are expected during the rather mild tempering of 5 minutes at 460°C.

It is well known that fresh lath martensite contains a high density of dislocations together with extreme internal stresses and that both of these are reduced on tempering. These can be quantified using measurements of X-ray diffraction line breadths and this method was applied to compare the as-quenched and annealed conditions of the present steels. Results for the (110) and (220) reflections are shown in Fig. 9 in the form of a Hall-Williamson plot. For clarity, only the high nitrogen steels, 2, 4 and 6, are shown here but others all behaved similarly. Lines through the measured points extrapolate very close to the origin which indicates that the source of line broadening

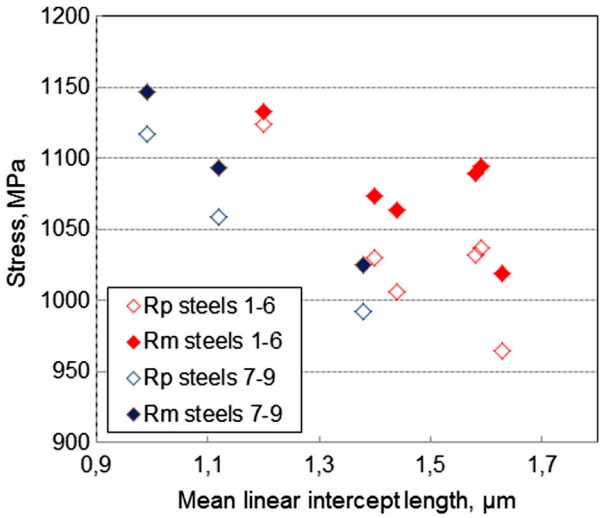

8 Yield and tensile stresses for steels heat treated 5 minutes at 460°C, plotted as a function of the mean linear intercept length of martensite boundaries having misorientations >15°

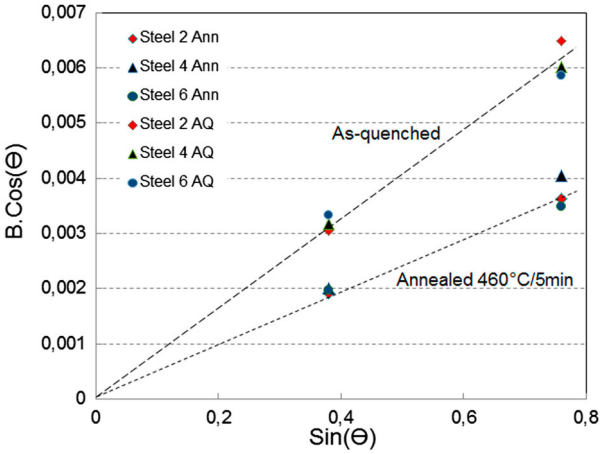

9 Hall-Williamson plot showing X-ray line broadening (B) for three steels in the as-quenched condition and after heat treating 5 minutes at 460°C

arises from inhomogeneous strain (dislocations and type II elastic strains) and that particle size effects are negligible. Relaxation of internal strains after heat treatment is very clear from the decrease in broadening and the reduced slopes of the lines. However, there is no effect of the different vanadium contents, either in the as-quenched conditions or after annealing. It may be concluded from this that vanadium does not inhibit the recovery of the fine scale internal structures of the martensite during these treatments and so a mechanism based on recovery is unlikely to explain the beneficial role of the microalloying that is observed.

Transmission electron microscopy was used to examine a sample of steel 6 (HV/HN) that had been annealed for 5 minutes at 460°C to simulate a galvanising treatment. The micrograph in Fig. 10*a* shows a typically dislocated martensitic structure with striations that appear to be lath boundaries, possibly decorated with carbon. It was difficult to identify second phase particles in the bright field images but scanning EDS pictures showed numerous examples of vanadium concentrations that are consistent with particles of about 25 nm diameter, Fig. 10*b*. These local V-concentrations were much greater than in the matrix. The most commonly occurring precipitate in V-microalloyed steels is the nitride VN which has the Baker-Nutting orientation relationship with ferrite and a lattice mis-match of only 2.1%.[6] Together with the small size of the particles, this may account for their poor image contrast. Nevertheless, the evidence that small V-containing particles do exist gives a possible explanation of the higher strength of the V-microalloyed steels after annealing.

APT was also used to investigate the occurrence and distribution of minor elements for steel 6 (HV/HN) in three conditions. These were as-quenched and with simulated galvanising 5 minutes at 460°C and the same after galvannealing 550°C for 15 seconds. The structure of the as-quenched steel shown in Fig. 11 was similar to examples from APT in the literature e.g.[8,13,14] Carbon is mainly segregated to lath boundaries and dislocations while other elements are homogeneously dispersed. Apparent enrichment of some other elements at the lath boundary in Fig. 11 is an artefact associated with an increased local density yield of ions and is not a true increased concentration.

Although several specimens of annealed steel were examined, these produced much smaller examined volumes due to the tips fracturing after short times, possibly due to weakness caused by the numerous cementite particles in the tempered structures. No examples of V-rich particles of the sort seen in TEM were found, probably because of these limited volumes that could be examined.

To test for possible clustering effects which might contribute to the increased strength in the presence of vanadium, distributions of 5th nearest-neighbour (5NN) distances of vanadium and nitrogen atoms were calculated and compared with the expected distributions in random solid solutions. Some of these results are shown in Fig. 12. The experimental and modelled (random) distributions coincide very closely in both the as-quenched and annealed conditions, suggesting that no measurable degree of clustering of the vanadium and nitrogen atoms exists in either condition. A similar conclusion was obtained when vanadium atoms alone were treated in the same type of analysis.

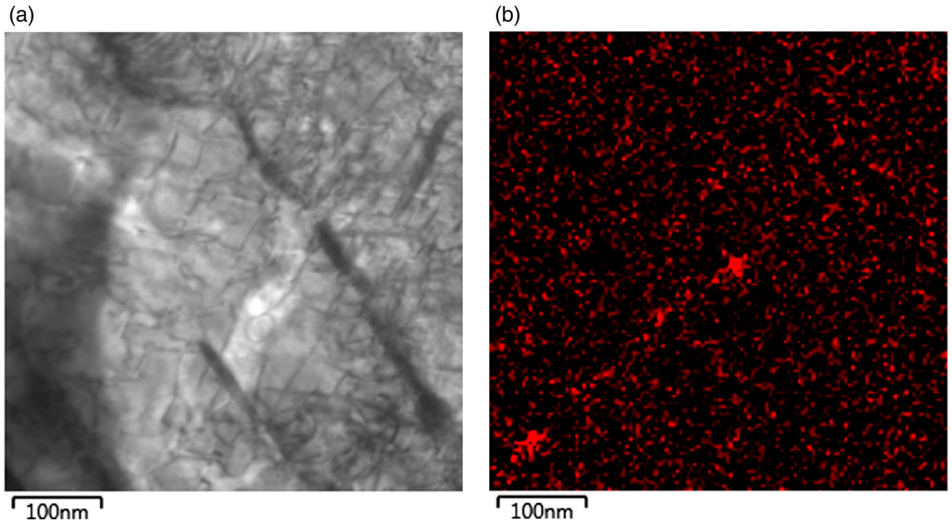

10 TEM images from Steel 6 after annealing for 5 minutes at 460°C, *a* bright field image, *b* EDS mapping with VKα energy

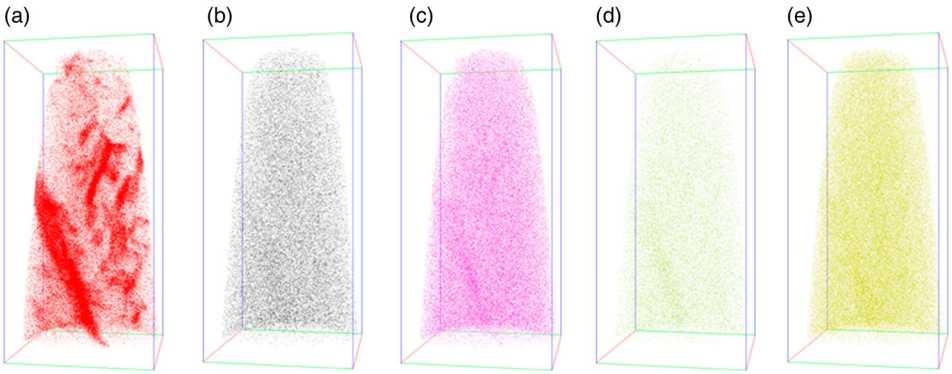

11 APT maps of elemental distributions for steel 6 in the as-quenched condition. *a* carbon, *b* vanadium, *c* chromium, *d* nitrogen and *e* manganese. Outline boxes are 100 nm × 100 nm in cross-section

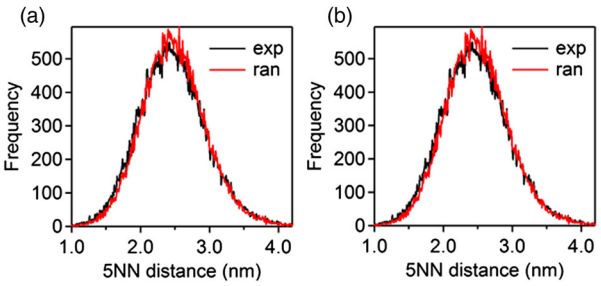

12 Comparison of experimental (exp) and modelled random (ran) distributions for V+N atoms for steel 6, *a* as-quenched and *b* quenched and annealed for 5 minutes at 460°C

Table 4 Elemental contents (wt-%) in the matrix of steel 6 in different heat treatment conditions

Condition	C%	N%	Al%	V%
As-quenched	0.199	0.013	0.021	0.092
Annealed 460°C for 5 min.	0.039	0.012	0.012	0.072
Annealed 460°C for 5 min. +550°C for 15 sec.	0.021	0.018	0.009	0.087
Bulk composition	0.199	0.0125	0.021	0.092

The annealed conditions showed low carbon contents in the matrix which can be explained by its redistribution to the relatively coarse cementite particles, Fig. 7*a*. Otherwise, no significant difference could be detected following the annealing treatments. However, some further information was obtained relating to the contents of alloying element ostensibly in solid solution in the steel matrix, presented in Table 4. The as-quenched results which have the largest statistical basis agree very well with the bulk analyses. Apart from the significant reduction in carbon level, annealing makes rather little difference but the contents are all significantly larger than the values calculated from ThermoCalc in Table 1. This indicates that the precipitation reactions leading to VN and AlN during annealing at 900°C for 3 minutes are quite far from the equilibrium state that is predicted by the model. Within the accuracy of these measurements there is no change in the matrix contents of vanadium or nitrogen after the simulated galvanising treatment.

Conclusions

The investigation was carried out to see whether microalloying with vanadium can improve the strength of hardened martensitic steel sheet after it is subjected to hot-dip metallising processes.

Useful increase in strength (>100 MPa) is achieved with vanadium additions and this is further enhanced in the presence of moderately raised nitrogen contents. In aluminium-killed steel, appropriate levels are around 0.05%V and 0.01%N. These apply for thermal cycles typical of hot-dip galvanising and also galvannealing and now merit industrial-scale validation.

Bendability of the sheets deteriorates somewhat as the strength level rises as commonly observed. However, changing the deoxidation treatment from aluminium to silicon gives two benefits. It allows a reduction in the nitrogen content since none of this is then consumed as aluminium nitride, and it significantly improves the bendability at a given strength level.

The reasons(s) why alloying with vanadium improves strength under these conditions is still not fully established. Recovery in the dislocated martensite is not affected by the presence of vanadium. There appears to be some contribution from refinement of the martensitic lath structure but the most probable reason is strengthening due to precipitates, believed to be VN, that were detected by TEM.

Acknowledgements

This research has been funded by Vanitec and the authors thank David Milbourn for his support and encouragement. Very significant contributions to the experimental programme were made by Christer Eggertson and Jacek Komenda, at SwereaKIMAB. We also thank Lena Ryde and David Lindell for useful discussions and acknowledge with gratitude Peter Hodgson for provision of facilities at Deakin University. APT experiments were carried out with the support of the Deakin University Advanced Characterisation Facility.

ORCiD

O. Karlsson http://orcid.org/0000-0003-4679-9535

References

1. D. Bhattacharya: 'Developments in advanced high strength steels', *Proc. Joint Int. Conf. HSLA Steels*, 2005, 70–73.
2. Y. Miyoshi: 'State of the art in precoated steel sheet for automotive body materials in Japan', *ISIJ Int.*, 1991, **31**, 1–10.
3. H. H. Lee and D. Hiam: 'Corrosion resistance of galvannealed steel', *Corrosion*, 1989, **45**, 852–856.
4. R. A. Grange, C. R. Hribal and L. F. Porter: 'Hardness of tempered martensite in carbon and low alloy steels', *Met. Trans.*, 1977, **8**, 1775–1785.
5. T. Siwecki, J. Eliasson, R. Lagneborg and B. Hutchinson: 'Vanadium microalloyed bainitic hot strip steels', *ISIJ Int.*, 2010, **50**, 760–767.
6. R. Lagneborg, W. B. Hutchinson, T. Siwecki and S. Zajac: 'The role of vanadium in microalloyed steels', ISBN 978-91-633-9359-4, SwereaKIMAB, 2014.
7. J. M. Long, D. A. Haynes and P. D. Hodgson: 'Characterisation of galvanneal coatings on strip steel materials', *Mater. Forum*, 2004, **27**, 62–67.
8. B. Hutchinson, J. Hagström, O. Karlsson, D. Lindell, M. Tornberg, F. Lindberg and M. Thuvander: 'Microstructures and hardness of as-quenched martensites (0.1 to 0.5%C)', *Acta Mater.*, 2011, **59**, 5845–5858.
9. B. Hutchinson, D. Lindell and M. Barnett: 'Yielding behaviour in martensite', *ISIJ Int.*, 2015, **55**, 1114–1122.
10. B. Gault, M. P. Moody, J. M. Cairney and S. P. Ringer: 'Atom probe microscopy', 2012, New York, Springer.
11. G. Krauss: 'Heat treated martensitic steels: microstructural systems for advanced manufacture', *ISIJ Int.*, 1995, **35**, 349–359.
12. E. I. Galindo-Nava and P. E. J. Rivera-Diaz-del-Castillo: 'A model for the microstructural behaviour and strength evolution in lath martensite', *Acta Mater.*, 2015, **98**, 81–93.
13. C. Zhu, A. Cerezo and G. D. W. Smith: 'Carbide characterisation in low-temperature tempered steels', *Ultramicroscopy*, 2009, **109**, 545–552.
14. E. V. Pereloma, K. F. Russell, M. K. Miller and I. B. Timokhina: 'Observations of decomposition of martensite during heat treatment of steels using atom probe tomography', *Scripta Mater.*, 2008, **58**, 1078–1081.